Relativistic many-body calculations of energies of $n=2$ states for boronlike ions

M. S. Safronova, W. R. Johnson, and U. I. Safronova*
Department of Physics, University of Notre Dame, Notre Dame, Indiana 46556
(Received 28 May 1996)

Energies of the fifteen $(2l2l'2l'')$ states for boronlike ions with $Z = 5$–100 are evaluated to second order in relativistic many-body perturbation theory. Second-order Coulomb and Breit-Coulomb interactions are included. Corrections are made to lowest order for the frequency-dependent Breit interaction and for the Lamb shift. A detailed discussion of the various contributions to the energy levels is given for boronlike iron ($Z=26$). Comparisons of the calculated energy levels with available experimental data are made for the entire sequence. [S1050-2947(96)09610-2]

PACS number(s): 31.15.Md, 31.25.Jf, 31.30.Jv

I. INTRODUCTION

Boronlike ions are simple atomic systems for which both three-electron interactions and interactions with an atomic core are important. Three-electron interactions play a dominant role, of course, for $(1s2lnl')$ autoionizing levels of lithiumlike ions; however, for such ions there are no core interactions [1,2]. Edlén, in his 1933 thesis [3], was perhaps the first to identify lines of boronlike ions. Fifty years later, he gave detailed comparisons of theoretical and experimental energies along the boron isoelectronic sequence [4]. On the basis of this comparison, he suggested a simple empirical formula to predict levels of high Z boronlike ions. This formula was used by Denne and Hinnov [5] to identify spectra obtained in high-temperature Tokamak plasmas. The five lines corresponding to $2s^22p-2s2p^2$ transitions for Ti XVIII, Cr XX, Fe XXII, and Ni XXIV were identified in spectra obtained from Princeton Large Torus tokamak plasmas by Dave *et al.* [6]. More recently, this sequence was extended to Mo XXXVIII by Myrnäs *et al.* [7]. Highly-charged uranium and thorium ions were produced in a high-energy electron beam ion trap (SuperEBIT) at Lawrence Livermore National Laboratory [8,9]. Thirteen $2s_{1/2}-2p_{3/2}$ transitions (Li-like through Ne-like uranium and thorium) were identified and measured with high accuracy. Experimental energies for boronlike ions obtained by different authors have been gathered and critically evaluated in Refs. [10–26]. Some of these energies are used below for comparison.

Nonrelativistic perturbation theory was used to calculate energies of $(2l2l'2l'')$ states for boronlike ions in Refs. [27–29]. Contributions of the Breit interaction, calculated using exact nonrelativistic wave functions, were expressed as a $1/Z$ expansion in Refs. [30,31]. By introducing screening constants, and including radiative and higher-order relativistic effects in this method (referred to as the MZ method), accurate predictions were obtained for ions in the range $Z = 6$–54 [30,31]. The multiconfiguration Dirac-Fock (MCDF) technique was used to calculate energies of the first excited states of boronlike ions with $Z=6$–92 in Ref. [32]. This MCDF calculation was improved for boronlike iron ($Z=26$) by adding the second-order correlation energy [33].

In the present paper, we use relativistic many-body perturbation theory (MBPT) to determine energies of $n=2$ states for boronlike ions with nuclear charges in the range $Z = 5$–100. We illustrate our calculation with detailed studies of the cases $Z=26$, 90, and 92. High-quality experimental data exist for each of these ions. We determine energies for the $(2s^22p)\ ^2P_{1/2}$ ground state, the six odd-parity $(2s^22p)\ ^2P_{3/2}$, $(2p^3)\ ^4S_{3/2}$, $(2p^3)\ ^2P_J$, $(2p^3)\ ^2D_J$ excited states, and the eight even-parity $(2s2p^2)$ $[^4P_J, ^2P_J, ^2D_J, ^2S_{1/2}]$ excited states. Our calculations are carried out to second order in perturbation theory and include both the second-order Coulomb interaction and the second-order Breit-Coulomb interaction. Correction for the frequency-dependent Breit interaction are taken into account in lowest order. The effect of the Lamb shift is estimated from a calculation in a local central potential that approximates the core HF potential. The three-electron contributions to the energy are compared with the one- and two-electron contributions. They are found to contribute about 30% of the total second-order energy.

Our perturbation theory calculations are carried out using single-particle orbitals calculated in the HF potential of the $(1s)^2$ heliumlike core. As a first step, we determine and store the single-particle contributions to the energy for the three $n=2$ states $(2s, 2p_{1/2}$, and $2p_{3/2})$ in lowest, first, and second orders. These contributions are precisely those needed to calculate energies of $n=2$ states of lithiumlike ions. Next, we evaluate and store the twenty possible two-particle matrix elements of the effective Hamiltonian, $\langle 2l2l'J|H^{\rm eff}|2l''2l'''J\rangle$, in first and second order. The one- and two-particle matrix elements were used previously to evaluate energies of the $(2l2l')$ levels for berylliumlike ions [34]. Finally, second-order three-particle matrix elements are evaluated. Combining these data using the method described below, we calculate one-, two-, and three-particle contributions to the energies of boronlike ions. To check correctness of the various terms in the energy matrix, we also evaluated all of the above contributions using relativistic Coulomb wave functions, and compared the individual terms with previous nonrelativistic calculations [29]. It should be emphasized that the methods used here for boronlike ions can be used as well to calculate energies of aluminumlike ions and similar three-valence electron systems.

*Permanent address: Institute for Spectroscopy, Russian Academy of Sciences, Troitsk 142092, Russia.

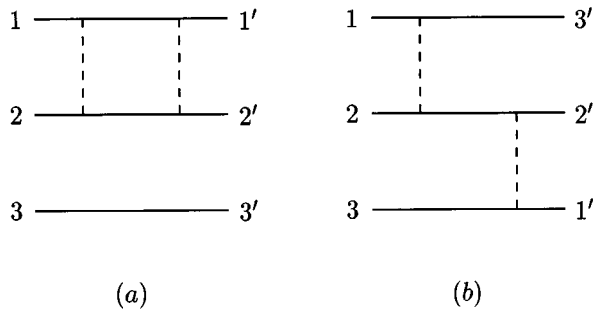

FIG. 1. Second-order diagrams: (a) two-particle diagram, (b) three-particle diagram.

The present calculations are compared with theoretical results from Ref. [33] for $Z=26$, and with the CI calculations of Chen and Cheng [35] for the $2s-2p_{3/2}$ transitions in boronlile thorium and uranium. Comparisons of the ionization potentials and multiplet splittings along the isoelectronic sequence with available experimental data are also given.

II. METHOD

The evaluation of the second-order energies for boronlike ions follows the pattern of the corresponding calculation for berylliumlike ions given in Ref. [34]. In particular, we use the second-order one- and two-particle matrix elements for berylliumlike ions calculated in [34], but recoupled as described below, to obtain the contributions from all diagrams of the type shown in Fig. 1(a). We will discuss how these matrix elements are combined to obtain the one- and two-particle contributions to energies of boronlike ions. We refer the reader to Ref. [34] for a discussion of how the basic one- and two-particle matrix elements were evaluated. Intrinsically three-particle diagrams of the type shown in Fig. 1(b) also contribute to the second-order energy for boronlike ions. We discuss the evaluation of these three-particle diagrams in detail. It should be noted that the three-particle matrix elements calculated here can also be used in calculations of energies of ions with four or more valence electrons.

The model space state vector for an ion with three valence electrons outside a closed core can be represented as [36]

$$\Psi(QJM)=N(Q)\sum \langle\beta_1\beta_2|K_{12}\rangle\langle K_{12}\beta_3|K\rangle a^\dagger_{\beta_1}a^\dagger_{\beta_2}a^\dagger_{\beta_3}|0\rangle, \tag{2.1}$$

where $|0\rangle$ is the state vector for the core ($1s^2$, in our case), Q describes a three-particle state with quantum numbers $n_1^0\kappa_1^0 n_2^0\kappa_2^0[J_{12}]n_3^0\kappa_3^0$, and intermediate momentum J_{12}. We use the notation $K_i=\{J_i,M_i\}$ and $\beta_i=\{j_i,m_i\}$. The sum in Eq. (2.1) is over magnetic quantum numbers m_1, m_2, m_3, and M_{12}. The quantity $\langle K_1K_2|K_3\rangle$ is a Clebsch-Gordan coefficient:

$$\langle K_1K_2|K_3\rangle=(-1)^{J_1-J_2+M_3}\sqrt{2J_3+1}\begin{pmatrix} J_1 & J_2 & J_3 \\ M_1 & M_2 & -M_3\end{pmatrix}. \tag{2.2}$$

The above representation of the state vector is somewhat inconvenient; for example, it leads to an expression containing 36 terms for the three-particle diagram in Fig. 1(b), differing only in the order of the initial and final indices. It is more efficient to express the state vector in a manifestly symmetric form. To this end, we rewrite Eq. (2.1) in six equivalent ways, merely permuting the indices β_1,β_2, and β_3. The resulting state vector is

$$\begin{aligned}\Psi(QJM)=\frac{1}{6}N(Q)\sum_{M_{12}\{\beta\}}[&\langle\beta_1\beta_2|K_{12}\rangle\langle K_{12}\beta_3|K\rangle\delta_{123}\\ &-\langle\beta_2\beta_1|K_{12}\rangle\langle K_{12}\beta_3|K\rangle\delta_{213}+\langle\beta_2\beta_3|K_{12}\rangle\\ &\times\langle K_{12}\beta_1|K\rangle\delta_{231}-\langle\beta_3\beta_2|K_{12}\rangle\langle K_{12}\beta_1|K\rangle\delta_{321}\\ &+\langle\beta_3\beta_1|K_{12}\rangle\langle K_{12}\beta_2|K\rangle\delta_{312}-\langle\beta_1\beta_3|K_{12}\rangle\\ &\times\langle K_{12}\beta_2|K\rangle\delta_{132}]a^\dagger_{\beta_1}a^\dagger_{\beta_2}a^\dagger_{\beta_3}|0\rangle,\end{aligned} \tag{2.3}$$

where $\{\beta\}$ ranges over the 3! permutations of the single-particle indices, and where

$$\delta_{123}=\delta(1,1^0)\,\delta(2,2^0)\,\delta(3,3^0).$$

Using the following angular momentum identity [37]:

$$\begin{aligned}&\sum_{M_{12}}\langle\beta_1\beta_3|K_{12}\rangle\langle K_{12}\beta_2|K\rangle\\ &=\sum_{J_{12}M_{12}}(-1)^{J_{12}+J''_{12}+j_3+j_2}\langle\beta_1\beta_2|K''_{12}\rangle\\ &\quad\times\langle K''_{12}\beta_3|K\rangle\sqrt{(2J_{12}+1)(2J''_{12}+1)}\begin{Bmatrix} j_2 & j_3 & J''_{12}\\ J_1 & J & J_{12}\end{Bmatrix},\end{aligned} \tag{2.4}$$

the three-particle state vector can be represented in a form

$$\Psi(QJM)=\sum_{\beta_1\beta_2\beta_3}C^{QJM}_{\beta_1\beta_2\beta_3}a^\dagger_{\beta_1}a^\dagger_{\beta_2}a^\dagger_{\beta_3}|0\rangle. \tag{2.5}$$

The factor $C^{QJM}_{\beta_1\beta_2\beta_3}$ provides the orthonormality and antisymmetry of the state vector in all one-electron (β_1,β_2, and β_3) indices. We may write

$$C^{QJM}_{\beta_1\beta_2\beta_3}=\sum_{K''_{12}}\langle\beta_1\beta_2|K''_{12}\rangle\langle K''_{12}\beta_3|K\rangle C_{11^022^033^0}(J_{12},J''_{12},J), \tag{2.6}$$

where the indices (1,2,3) designate $(n_1\kappa_1,n_2\kappa_2,n_3\kappa_3)$, and where the indices $(1^0,2^0,3^0)$ designate $(n_1^0\kappa_1^0,n_2^0\kappa_2^0,n_3^0\kappa_3^0)$. We note that the dependence on magnetic quantum numbers is included in the two Clebsch-Gordan coefficients, and all permutations of the three indices are in the factor $C_{11^022^033^0}(J_{12},J''_{12},J)$, which is independent of magnetic quantum numbers. One finds

TABLE I. Contributions to the second-order matrix elements for B-like iron ($Z=26$) in a.u. In columns 3–8, the number in square brackets denotes the power of 10.

Matrix element		$E_1^{(2)}$	$E_2^{(2)}$	$E_3^{(2)}$	$B_1^{(2)}$	$B_2^{(2)}$	$B_3^{(2)}$
			$J=1/2$ odd				
$2s2s[0]2p^*$	$2s2s[0]2p^*$	-0.264827[-1]	-0.127850[-0]	-0.656374[-1]	-0.308971[-2]	-0.533118[-2]	-0.214070[-3]
$2p2p[0]2p^*$	$2p2p[0]2p^*$	-0.382312[-1]	-0.218904[-0]	-0.112379[-0]	-0.365215[-2]	-0.887883[-2]	-0.926460[-3]
$2s2s[0]2p^*$	$2p2p[0]2p^*$		0.332192[-1]	0.956959[-2]		0.130290[-2]	0.108640[-3]
$2p2p[0]2p^*$	$2s2s[0]2p^*$		0.315634[-1]	0.106161[-1]		0.123260[-2]	0.177300[-3]
			$J=3/2$ odd				
$2s2s[0]2p$	$2s2s[0]2p$	-0.257007[-1]	-0.127675[-0]	-0.651486[-1]	-0.289492[-2]	-0.418533[-2]	-0.261970[-3]
$2p2p[2]2p^*$	$2p2p[2]2p^*$	-0.382312[-1]	-0.162226[-0]	-0.971880[-1]	-0.365215[-2]	-0.717588[-2]	-0.644260[-3]
$2p^*2p^*[0]2p$	$2p^*2p^*[0]2p$	-0.390131[-1]	-0.195739[-0]	-0.106181[-0]	-0.384695[-2]	-0.947643[-2]	-0.509780[-3]
$2p2p[0]2p$	$2p2p[0]2p$	-0.374492[-1]	-0.193442[-0]	-0.104371[-0]	-0.345736[-2]	-0.652149[-2]	-0.729410[-3]
$2s2s[0]2p$	$2p2p[2]2p^*$		0.000000[-0]	-0.192200[-4]		0.000000[-0]	0.282300[-4]
$2p2p[2]2p^*$	$2s2s[0]2p$		0.000000[-0]	-0.192300[-4]		0.000000[-0]	-0.800000[-6]
$2s2s[0]2p$	$2p^*2p^*[0]2p$		0.230278[-1]	0.650344[-2]		0.717040[-3]	0.599800[-4]
$2p^*2p^*[0]2p$	$2s2s[0]2p$		0.221848[-1]	0.701846[-2]		0.691767[-3]	0.249500[-4]
$2s2s[0]2p$	$2p2p[0]2p$		0.234895[-1]	0.663667[-2]		0.921288[-3]	0.315600[-4]
$2p2p[0]2p$	$2s2s[0]2p$		0.223187[-1]	0.736370[-2]		0.871577[-3]	0.124560[-3]
$2p2p[2]2p^*$	$2p^*2p^*[0]2p$		0.254259[-1]	0.438694[-2]		0.508236[-3]	0.997000[-4]
$2p^*2p^*[0]2p$	$2p2p[2]2p^*$		0.256835[-1]	0.432405[-2]		0.512042[-3]	0.984100[-4]
$2p2p[2]2p^*$	$2p2p[0]2p$		-0.256835[-1]	-0.426731[-2]		-0.512042[-3]	-0.921400[-4]
$2p2p[0]2p$	$2p2p[2]2p^*$		-0.254259[-1]	-0.432948[-2]		-0.508236[-3]	-0.934000[-4]
$2p^*2p^*[0]2p$	$2p2p[0]2p$		-0.244734[-1]	-0.661120[-2]		-0.965367[-3]	-0.124170[-3]
$2p2p[0]2p$	$2p^*2p^*[0]2p$		-0.240675[-1]	-0.680506[-2]		-0.950471[-3]	-0.127420[-3]
			$J=5/2$ odd				
$2p2p[2]2p^*$	$2p2p[2]2p^*$	-0.382312[-1]	-0.202427[-0]	-0.103899[-0]	-0.365215[-2]	-0.676242[-2]	-0.478100[-4]
			$J=1/2$ even				
$2p^*2p^*[0]2s$	$2p^*2p^*[0]2s$	-0.331389[-1]	-0.159046[-0]	-0.682029[-1]	-0.356572[-2]	-0.828600[-2]	-0.329890[-3]
$2p2p[0]2s$	$2p2p[0]2s$	-0.315750[-1]	-0.182036[-0]	-0.634433[-1]	-0.317614[-2]	-0.654263[-2]	-0.705540[-3]
$2p^*2p[1]2s$	$2p^*2p[1]2s$	-0.323569[-1]	-0.172328[-0]	-0.777728[-1]	-0.337093[-2]	-0.671150[-2]	-0.360550[-3]
$2p^*2p^*[0]2s$	$2p2p[0]2s$		-0.346106[-1]	0.502457[-2]		-0.136524[-2]	-0.137040[-3]
$2p2p[0]2s$	$2p^*2p^*[0]2s$		-0.340366[-1]	0.511516[-2]		-0.134417[-2]	-0.158010[-3]
$2p^*2p^*[0]2s$	$2p^*2p[1]2s$		-0.442981[-1]	-0.747114[-2]		-0.727879[-3]	0.595100[-4]
$2p^*2p[1]2s$	$2p^*2p^*[0]2s$		-0.439120[-1]	-0.756248[-2]		-0.724006[-3]	0.842000[-5]
$2p2p[0]2s$	$2p^*2p[1]2s$		0.310505[-1]	0.551654[-2]		0.511949[-3]	0.970000[-5]
$2p^*2p[1]2s$	$2p2p[0]2s$		0.313235[-1]	0.544749[-2]		0.514688[-3]	-0.384200[-4]
			$J=3/2$ even				
$2p^*2p[1]2s$	$2p^*2p[1]2s$	-0.323569[-1]	-0.114922[-0]	-0.678492[-1]	-0.337093[-2]	-0.573764[-2]	-0.327400[-3]
$2p^*2p[2]2s$	$2p^*2p[2]2s$	-0.323569[-1]	-0.185428[-0]	-0.711031[-1]	-0.337093[-2]	-0.620816[-2]	-0.152680[-3]
$2p2p[2]2s$	$2p2p[2]2s$	-0.315750[-1]	-0.187786[-0]	-0.753208[-1]	-0.317614[-2]	-0.531738[-2]	-0.313460[-3]
$2p^*2p[1]2s$	$2p^*2p[2]2s$	0.246557[-1]	0.424196[-2]		0.320937[-3]	-0.127780[-3]	
$2p^*2p[2]2s$	$2p^*2p[1]2s$	0.246557[-1]	0.424196[-2]		0.320937[-3]	-0.401400[-4]	
$2p^*2p[1]2s$	$2p2p[2]2s$	-0.350208[-1]	-0.592824[-2]		-0.575439[-3]	0.960200[-4]	
$2p2p[2]2s$	$2p^*2p[1]2s$	-0.347155[-1]	-0.600247[-2]		-0.572377[-3]	-0.401800[-4]	
$2p^*2p[2]2s$	$2p2p[2]2s$	0.415499[-2]	0.700561[-2]		-0.122510[-4]	-0.651800[-4]	
$2p2p[2]2s$	$2p^*2p[2]2s$	0.414890[-2]	0.709114[-2]		-0.112190[-4]	-0.481000[-4]	
			$J=5/2$ even				
$2p^*2p[2]2s$	$2p^*2p[2]2s$	-0.323569[-1]	-0.153411[-0]	-0.654774[-1]	-0.337093[-2]	-0.541372[-2]	0.109000[-3]
$2p2p[2]2s$	$2p2p[2]2s$	-0.315750[-1]	-0.123939[-0]	-0.643519[-1]	-0.317614[-2]	-0.410860[-2]	-0.130290[-3]
$2p^*2p[2]2s$	$2p2p[2]2s$		-0.410566[-1]	-0.628030[-3]		-0.755139[-3]	-0.636100[-4]
$2p2p[2]2s$	$2p^*2p[2]2s$		-0.406686[-1]	-0.637420[-3]		-0.750154[-3]	-0.825600[-4]

$$C_{11^0 22^0 33^0}(J_{12},J''_{12},J)=N(1^0,2^0,3^0)\Bigg[\delta(3,3^0)\,\delta(J_{12},J''_{12})P_{J_{12}}(11^0,22^0)$$
$$+\delta(3,1^0)P_{J''_{12}}(13^0,22^0)\sqrt{(2J_{12}+1)(2J''_{12}+1)}\begin{Bmatrix} j_3^0 & j_2^0 & J''_{12}\\ j_1^0 & J & J_{12}\end{Bmatrix}$$
$$+\delta(3,2^0)P_{J2'_{12}}(13^0,21^0)\sqrt{(2J_{12}+1)(2J''_{12}+1)}\begin{Bmatrix} j_3^0 & j_1^0 & J''_{12}\\ j_2^0 & J & J_{12}\end{Bmatrix}(-1)^{j_1^0+j_2^0+J_{12}}\Bigg], \qquad (2.7)$$

where

$$P_{J_{12}}(11^0,22^0)=\delta(1,1^0)\,\delta(2,2^0)$$
$$+(-1)^{j_1^0+j_2^0+J_{12}+1}\delta(1,2^0)\,\delta(2,1^0). \quad (2.8)$$

Here, we have used $N(1^0,2^0,3^0)$ instead of $N(Q)$ to designate the normalization factor, which can be obtained from

$$\sum_{1,2,3,J''_{12}}(C_{11^0 22^0 33^0}(J_{12},J''_{12},J))^2=6. \qquad (2.9)$$

Using this representation it is possible to express contributions of diagrams of the type shown in Fig. 1(a) in terms of the energy matrix elements for two-electron (berylliumlike) ions. Moreover, with this representation, only one expression is needed to evaluate the contributions from the diagram in Fig. 1(b).

The model space for $n=2$ states of boronlike ions consists of seven odd parity states consisting of two $J=1/2$ states, four $J=3/2$ states, and one $J=5/2$ state and eight even parity states consisting of three $J=1/2$ states, three $J=3/2$ states, and two $J=5/2$ states which can be summarized as follows:

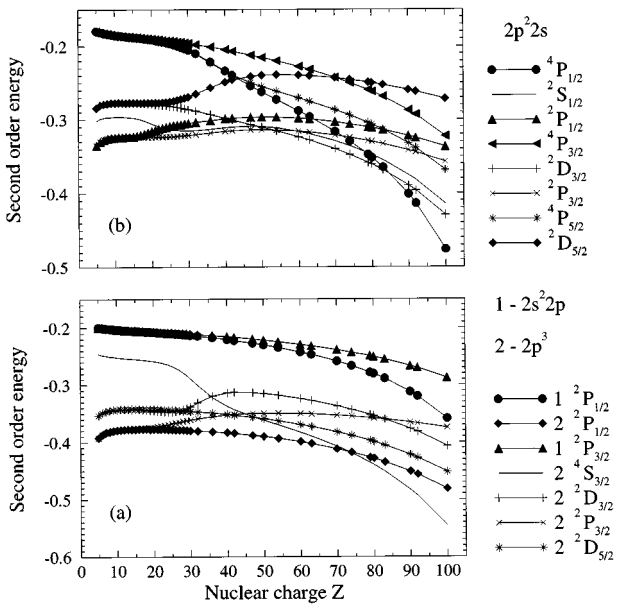

FIG. 2. Second-order energy contributions: (a) odd-parity states, (b) even-parity states.

Odd parity states:

$J=1/2$	$J=3/2$	$J=5/2$
$2s_{1/2}2s_{1/2}[0]2p_{1/2}$	$2s_{1/2}2s_{1/2}[0]2p_{3/2}$	$2p_{3/2}2p_{3/2}[2]2p_{1/2}$
$2p_{3/2}2p_{3/2}[0]2p_{1/2}$	$2p_{3/2}2p_{3/2}[2]2p_{1/2}$	
	$2p_{1/2}2p_{1/2}[0]2p_{3/2}$	
	$2p_{3/2}2p_{3/2}[0]2p_{3/2}$	

Even parity states:

$J=1/2$	$J=3/2$	$J=5/2$
$2p_{1/2}2p_{1/2}[0]2s_{1/2}$	$2p_{1/2}2p_{3/2}[1]2s_{1/2}$	$2p_{1/2}2p_{3/2}[2]2s_{1/2}$
$2p_{3/2}2p_{3/2}[0]2s_{1/2}$	$2p_{1/2}2p_{3/2}[2]2s_{1/2}$	$2p_{3/2}2p_{3/2}[2]2s_{1/2}$
$2p_{1/2}2p_{3/2}[1]2s_{1/2}$	$2p_{3/2}2p_{3/2}[2]2s_{1/2}$	

Let us now consider the coefficients $C_{11^0 22^0 33^0}(J_{12},J''_{12},J)$ for boronlike ions. To simplify the formulas the following notation is used:

$$C_J(1^0 2^0 J_{12} 3^0)\equiv C_{11^0 22^0 33^0}(J_{12},J''_{12},J),$$

$$Q_J(1^0 2^0 3^0)\equiv C_{11^0 22^0}(J)\,\delta(3,3^0),$$

$$C_{11^0 22^0}(J)=\eta_{12}P_{J_{12}}(11^0,22^0),$$

$$s\equiv 2s, \quad p^*\equiv 2p_{1/2}, \quad p\equiv 2p_{3/2},$$

where η is equal to 1 for nonequivalent electrons and $1/\sqrt{2}$ for equivalent ones. We then obtain the following from Eq. (2.7):

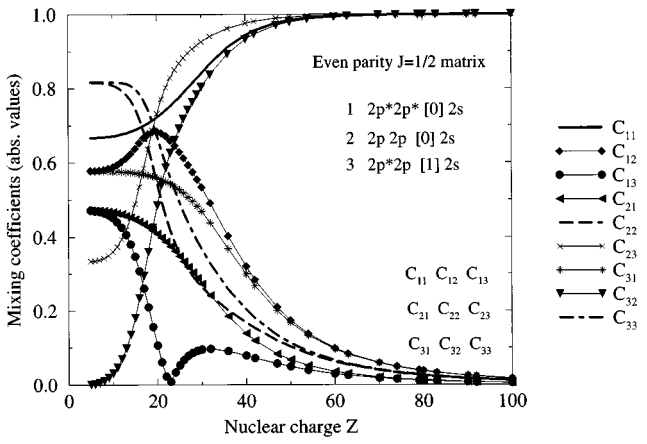

FIG. 3. Mixing coefficients for the even-parity $J=1/2$ states.

TABLE II. Energies of boronlike iron ($Z=26$) given relative to the ground state. Notation: $E^{(0+1)}=E^{(0)}+E^{(1)}+B^{(1)}$.

	$2p^2 2s$							
	$^4P_{1/2}$	$^4P_{3/2}$	$^4P_{5/2}$	$^2D_{3/2}$	$^2D_{5/2}$	$^2S_{1/2}$	$^2P_{1/2}$	$^2P_{3/2}$
$E^{(0+1)}$	405724.5	460002.8	513306.5	755414.7	776375.5	880272.2	1003367.4	1019967.5
$E^{(2)}$	2844.4	3854.5	3202.0	-15682.1	-14019.2	-22580.8	-21341.0	-24596.3
$B^{(2)}$	-367.2	-153.3	222.8	-280.1	-96.7	-812.9	-586.9	-220.1
$E_{\rm Lamb}$	-3652.3	-3490.9	-3389.3	-3459.5	-3349.8	-3585.0	-3289.4	-3297.8
$E_{\rm Tot}$	404549	460213	513342	735993	758910	853294	978150	991853
$E_{\rm Th}$ [33]	404691	459796	513373	735763	757578	858011	972713	990281
$E_{\rm Expt}$ [22]	404550	460200	513260	736520	759620	853480	978220	992290
	$2s^2 2p$	$2p^3$	$2p^3$	$2p^3$	$2p^3$	$2p^3$		
	$^2P_{3/2}$	$^4S_{3/2}$	$^2D_{3/2}$	$^2D_{5/2}$	$^2P_{1/2}$	$^2P_{3/2}$		
$E^{(0+1)}$	117397.9	1276431.5	1433133.0	1462519.3	1613924.3	1668716.6		
$E^{(2)}$	362.3	-13059.3	-29672.0	-29331.4	-36797.0	-34165.1		
$B^{(2)}$	264.9	-651.4	-1001.6	-467.5	-1191.0	-812.2		
$E_{\rm Lamb}$	241.9	-7258.3	-7241.0	-7169.8	-7018.1	-6821.5		
$E_{\rm Tot}$	118267	1255463	1395219	1425551	1568918	1626918		
$E_{\rm Th}$ [33]	118104	1256290	1395305	1425808	1569053	1626110		
$E_{\rm Expt}$ [22]	118270	1255700	1396410	1426880	1569630	1627720		

$2s^2 2p$ configuration,

$$C_{1/2}(ss0p^*)=Q_0(ssp^*)-\frac{1}{\sqrt{2}}Q_0(p^*ss)+\sqrt{\frac{3}{2}}Q_1(p^*ss),$$

$$C_{3/2}(ss0p)=Q_0(ssp)-\frac{\sqrt{3}}{2}Q_1(pss)+\frac{\sqrt{5}}{2}Q_2(pss).$$

$2p^3$ configuration,

$$C_{1/2}(pp0p^*)=Q_0(ppp^*)-\frac{\sqrt{3}}{2}Q_1(p^*pp)+\frac{\sqrt{5}}{2}Q_2(p^*pp),$$

$$C_{5/2}(pp2p^*)=Q_2(ppp^*)-\frac{1}{2}Q_1(p^*pp)+\frac{\sqrt{7}}{2}Q_2(p^*pp),$$

$$C_{3/2}(pp2p^*)=Q_2(ppp^*)-\sqrt{\frac{3}{2}}Q_1(p^*pp)-\frac{1}{\sqrt{2}}Q_2(p^*pp),$$

$$C_{3/2}(p^*p^*0p)=Q_0(p^*p^*p)-\frac{\sqrt{3}}{2}Q_1(p^*pp^*)+\frac{\sqrt{5}}{2}Q_2(p^*pp^*),$$

$$C_{3/2}(pp0p)=\frac{1}{\sqrt{2}}Q_0(ppp)-\sqrt{\frac{5}{2}}Q_2(ppp).$$

$2p^2 2s$ configuration,

$$C_{1/2}(p^*p^*0s)=Q_0(p^*p^*s)-\frac{1}{\sqrt{2}}Q_0(sp^*p^*)+\sqrt{\frac{3}{2}}Q_1(sp^*p^*),$$

$$C_{1/2}(pp0s)=Q_0(pps)-\frac{\sqrt{3}}{2}Q_1(spp)+\frac{\sqrt{5}}{2}Q_2(spp),$$

$$C_{1/2}(p^*p1s)=Q_1(p^*ps)-Q_1(spp^*)-Q_1(sp^*p),$$

$$C_{3/2}(p^*p1s)=Q_1(p^*ps)-\frac{1}{4}Q_1(spp^*)+\frac{\sqrt{15}}{4}Q_2(spp^*)-\sqrt{\frac{3}{8}}Q_0(sp^*p)+\sqrt{\frac{5}{8}}Q_1(sp^*p),$$

$$C_{3/2}(p^*p2s)=Q_2(p^*ps)+\frac{\sqrt{15}}{4}Q_1(spp^*)+\frac{1}{4}Q_2(spp^*)$$

TABLE III. Comparison of the present MBPT calculations with CI calculations for B-like uranium and with experimental data for B-like uranium and B-like thorium for $2s_{1/2}-2p_{3/2}$ transitions.

	B-like thorium		B-like uranium	
	B-1	B-2	B-1	B-2
$E^{(0+1)}$	4127.278	4127.315	4561.882	4562.111
$E^{(2)}$	-2.102	-1.716	-2.072	-1.682
$B^{(2)}$	-0.176	-0.492	-0.154	-0.489
$E_{\rm Lamb}$	-35.632	-35.633	-38.826	-38.827
$E_{\rm Tot}$	4089.629	4089.473	4520.829	4521.113
$E_{\rm Expt}$[8,9]	4089.92	4089.92	4521.39	4521.39
$E_{\rm Th}$ (CI-DS) [35]			4521.30	4521.53
$E_{\rm Th}$ (CI-DH) [35]				4521.36

$$-\sqrt{\frac{5}{8}}Q_0(sp^*p)-\sqrt{\frac{3}{8}}Q_1(sp^*p),$$

$$C_{3/2}(pp2s)=Q_2(pps)-\sqrt{\frac{3}{2}}Q_1(spp)-\frac{1}{\sqrt{2}}Q_2(spp),$$

$$C_{5/2}(p^*p2s)=Q_2(p^*ps)-Q_2(spp^*)+Q_1(sp^*p),$$

$$C_{5/2}(pp2s)=Q_2(pps)-\frac{1}{2}Q_1(spp)+\frac{\sqrt{7}}{2}Q_2(spp).$$

Using this representaion, the expression for the energy matrix element for diagrams of the type Fig. 1(a) (which we designate by R) can be written

$$\begin{aligned}E^R(1^02^0[J_{12}]3^0J,1'^02'^0[J'_{12}]3'^0J)&=\sum_{1,2,1',2'}\sum_{J''_{12}}E^R(12,2'1',J)N(12)N(1'2')\\&\times\sum_3 C_{11^02^03^03^0}(J_{12},J''_{12},J)\\&\times C_{1'1'^02'2'^03'3'^0}(J'_{12},J''_{12},J),\end{aligned}\tag{2.10}$$

where $E^R(12,1'2',J)$ is the two-particle contribution to the $n_1\kappa_1n_2\kappa_2n_{1'}\kappa_{1'}n_{2'}\kappa_{2'}$ J matrix element for berylliumlike ions. Here, $N(12)=1/\sqrt{2}$ if electrons 1 and 2 are equivalent and 1/2 if they are not equivalent. This choice accounts for the fact that $E^R(12,1'2',J)$ contains both direct and exchange contributions.

The three-electron coefficients given by Eqs. (2.6) and (2.7) allow us to obtain the expression for the diagram of Fig. 1(b), designated by G. The contribution of this diagram to the second-order matrix elements takes the form

$$\begin{aligned}E^G(1^02^0[J_{12}]3^0J,1'^02'^0[J'_{12}]3'^0J)&=\sum_{1,2,3,1',2',3'}\sum_n\frac{v_{123'n}v_{1'2'3n}}{\epsilon_n+\epsilon_{3'}-\epsilon_1-\epsilon_2}C^{QJM}_{123}C^{Q'JM}_{1'2'3'},\end{aligned}\tag{2.11}$$

where $v_{ijkl}=g_{ijkl}+b_{ijkl}$ is the sum of the two-particle Coulomb matrix element g_{ijkl}, and the two-particle matrix element of instantaneous Breit interaction, b_{ijkl}. Carrying out angular reduction we obtain for Coulomb interaction [from the gg term in Eq. (2.11)]

$$\begin{aligned}E^G(1^02^0[J_{12}]3^0J,1'^02'^0[J'_{12}]3'^0J)&=-\sum_{1,2,3,1',2',3'}\sum_{J''_{12},J'''_{12}}\sum_{kk'}\\&\times(-1)^{j_2+j_{2'}-j_3-j_{3'}+J''_{12}+J'''_{12}+k+k'}\\&\times\sum_n\frac{X_k(123'n)X_k(1'2'3n)}{\epsilon_n+\epsilon_{3'}-\epsilon_1-\epsilon_2}\begin{Bmatrix}j_n & j_{3'} & J''_{12}\\ j_1 & j_2 & k\end{Bmatrix}\\&\times\begin{Bmatrix}j_n & j_3 & J\\ j_{1'} & j_{2'} & k'\end{Bmatrix}\begin{Bmatrix}J'''_{12} & j_{3'} & J\\ J''_{12} & j_3 & j_n\end{Bmatrix}\\&\times\sqrt{(2J''_{12}+1)(2J'''_{12}+1)}C_{11^02^03^03^0}(J_{12},J'''_{12},J),\\&\times C_{1'1'^02'2'^03'3'^0}(J'_{12},J'''_{12},J),\end{aligned}\tag{2.12}$$

where

$$X_k(abcd)=(-1)^k\langle a||C_k||c\rangle\langle b||C_k||d\rangle R_k(abcd)\tag{2.13}$$

(see for details [34]). We obtain a similar term for Breit contribution from linear terms $(gb+bg)$ of Eq. (2.11) by changing $X_k(123'_n)X_k(1'2'3n)$ to $X^B_k(123'n)X_k(1'2'3n)+X_k(123'n)X^B_k(1'2'3n)$ in Eq. (2.12). The expression for $X^B_k(abcd)$ is given in [38]. We see that the contribution of the G diagram is determined by a sum over the single-particle spectrum n (with restrictions for states with principal quantum number 2).

III. RESULTS AND DISCUSSION

We calculate energies of the 15 possible $(2l2l'2l'')$ $[J]$ states for all boronlike ions with nuclear charges $Z\leqslant 30$ and for 17 representative ions with $Z>30$ (Z = 32, 36, 40, 42, 47, 50, 54, 60, 63, 70, 74, 79, 80, 83, 90, 92, 100). These calculations include first- and second-order contributions from the Coulomb and Breit operators for the 43 possible matrix elements. Although the calculations presented here were carried out in a HF basis, calculations were also made using a relativistic Coulomb basis in order to compare our results with previous nonrelativistic calculations [27].

In Table I and in Figs. 2 and 3, we give details of our calculations of the first- and second-order contributions to the energy matrices. We list the contributions from one-, two-, and three-electron diagrams for $Z=26$. The columns headed $E^{(2)}_i$ and $B^{(2)}_i$ contain second-order contributions from the Coulomb and Breit operators, respectively. The columns headed $E^{(2)}_1$ and $B^{(2)}_1$ contain the total contributions from valence diagrams found in our previous paper [34]. Those headed $E^{(2)}_2$ and $B^{(2)}_2$ contain values obtained using data for two-electron diagrams given in [34] and recoupled according to Eq. (2.10). Contributions of the three-electron diagram are given in the columns $E^{(2)}_3$ and $B^{(2)}_3$. These values were obtained from Eq. (2.12) . We can see from Table I that the contributions of the three-electron diagram to the Coulomb energy are smaller by a factor of 2–3 than the two-electron contributions, but 2–3 times larger than the one-electron contributions. It should be noted that one- and two-electron contributions vanish for the $2s2s[0]2p-2p2p[2]2p^*$ matrix element, so the entire contribution is from the three-electron diagram. The contributions of the three-electron diagram to the Breit energy are smaller than those of the one- and two-electron diagrams.

Let us describe in more detail the calculation of $E^{(2)}_1$, $E^{(2)}_2$, $B^{(2)}_1$, and $B^{(2)}_2$. Consider, as an example, the (simplest) case of the $2s^2[0]2p^*[0]$ diagonal matrix element. In this case only two one-particle ($2s$ and $2p^*$) and three two-particle ($2s^2-2s^2$ $[J=0]$, $2s2p^*-2s2p^*$ $[J=0]$, and

TABLE IV. Energies of boronlike ions given relative to the ground state in cm^{-1} for ions with Z=5-42.

Z		$2p^2 2s\ {}^4P_{1/2}$	$2p^2 2s\ {}^2D_{3/2}$	$2p^2 2s\ {}^2S_{1/2}$	$2p^2 2s\ {}^2P_{1/2}$	$2p^3\ {}^4S_{3/2}$	$2p^3\ {}^2D_{3/2}$	$2p^3\ {}^2P_{1/2}$
5	$E_{\rm Tot}$	29688	46783	64495	72466	97144	95096	110234
	$E_{\rm Expt}$	28805	47857	63561	72535	97037		
6	$E_{\rm Tot}$	43768	73694	98361	108920	142227	148761	170231
	$E_{\rm Expt}$	43000	74933	96494	110625	142024	150468	168732
7	$E_{\rm Tot}$	57910	100019	131688	144248	187061	201517	229284
	$E_{\rm Expt}$	57187	101031	131003	145876	186797	203089	230404
8	$E_{\rm Tot}$	72107	126110	164788	179035	231813	253873	287900
	$E_{\rm Expt}$	71177	126950	164367	180481	231275	255186	289016
9	$E_{\rm Tot}$	86402	152184	197866	213598	276685	306167	346422
	$E_{\rm Expt}$	86035	152898	197565	214881	276657	307273	347418
10	$E_{\rm Tot}$	100852	178402	231081	248143	321870	358656	405118
	$E_{\rm Expt}$	99030	179020	230851	249292		359601	406001
11	$E_{\rm Tot}$	115515	204905	264566	282832	367556	411564	464220
	$E_{\rm Expt}$	114978	205412	264400	283869	367290	412395	465101
12	$E_{\rm Tot}$	130456	231825	298437	317814	413932	465095	523944
	$E_{\rm Expt}$	129890	232274	298282	318721	413610	465818	524652
13	$E_{\rm Tot}$	145740	259294	332800	353243	461194	519449	584508
	$E_{\rm Expt}$	144420	259730	332710	354080	460070	520140	585180
14	$E_{\rm Tot}$	161437	287448	367741	389298	509543	574823	646133
	$E_{\rm Expt}$	161010	287850	367670	390040	509330	575450	646760
15	$E_{\rm Tot}$	177615	316429	403328	426192	559190	631412	709051
	$E_{\rm Expt}$	177177	316807	403322	426877	558973	631961	709666
16	$E_{\rm Tot}$	194343	346383	439600	464181	610354	689411	773506
	$E_{\rm Expt}$	193882	346700	439580	464759	610075	689910	774020
17	$E_{\rm Tot}$	211690	377464	476579	503570	663262	749016	839759
	$E_{\rm Expt}$		377831	476636	504092			840411
18	$E_{\rm Tot}$	229722	409831	514276	544694	718148	810423	908086
	$E_{\rm Expt}$		410189	514410	545209			
19	$E_{\rm Tot}$	248502	443651	552723	587905	775248	873834	978784
	$E_{\rm Expt}$	248320	443960	552860	588260	775280	874320	979270
20	$E_{\rm Tot}$	268105	479112	592007	633568	834838	939494	1052202
	$E_{\rm Expt}$	267990	479420	592180	633760	834860	940000	1052700
21	$E_{\rm Tot}$	288524	516334	632182	681964	897032	1007515	1128560
	$E_{\rm Expt}$	288440	516640	632370	682250	897130	1008100	1129060
22	$E_{\rm Tot}$	309856	555555	673456	733494	962171	1078270	1208327
	$E_{\rm Expt}$		555860	673714	733749		1078790	1208810
23	$E_{\rm Tot}$	332114	596940	715991	788491	1030423	1152024	1291840
	$E_{\rm Expt}$	332180	597291	716370	788850	1030850	1152900	1292800
24	$E_{\rm Tot}$	355315	640680	759992	847330	1101966	1229135	1379497
	$E_{\rm Expt}$	354570	640932	760400	847750	1101840	1229660	1380270
25	$E_{\rm Tot}$	379460	686959	805675	910398	1176935	1310022	1471700
	$E_{\rm Expt}$	379660	687540	805930	910880	1177430	1310890	1472410
26	$E_{\rm Tot}$	404549	735993	853294	978150	1255463	1395219	1568918
	$E_{\rm Expt}$	404550	736520	853480	978220	1255700	1396410	1569630
27	$E_{\rm Tot}$	430559	787984	903107	1051036	1337615	1485310	1671608
	$E_{\rm Expt}$	431560	788520	903260	1050860	1338760	1486350	1672130
28	$E_{\rm Tot}$	457458	843156	955402	1129555	1423449	1580975	1780274
	$E_{\rm Expt}$	457980	843710	955660	1129490	1424810	1581860	1781090
29	$E_{\rm Tot}$	485190	901719	1010468	1214208	1512978	1682906	1895403
	$E_{\rm Expt}$	485730				1513780		
30	$E_{\rm Tot}$	513713	963929	1068640	1305561	1606287	1791874	2017564
	$E_{\rm Expt}$		964320	1068147				
32	$E_{\rm Tot}$	572850	1100290	1195653	1510677	1804678	2033832	2285238

TABLE IV. (*Continued*)

Z		$2p^2 2s\ {}^4P_{1/2}$	$2p^2 2s\ {}^2D_{3/2}$	$2p^2 2s\ {}^2S_{1/2}$	$2p^2 2s\ {}^2P_{1/2}$	$2p^3\ {}^4S_{3/2}$	$2p^3\ {}^2D_{3/2}$	$2p^3\ {}^2P_{1/2}$
	$E_{\rm Expt}$		1100600	1196000	1511320			
36	$E_{\rm Tot}$	697620	1428896	1502865	2028461	2255499	2633444	2931644
	$E_{\rm Expt}$	698000	1429450	1502900	2029440			
40	$E_{\rm Tot}$	828049	1850020	1902681	2727792	2798252	3424488	3763936
42	$E_{\rm Tot}$	894668	2103072	2145987	3161519	3112921	3906990	4265712
	$E_{\rm Expt}$	894050	2102900	2147300	3164770			

$2s2p^*-2s2p^*$ $[J=1]$) contributions are necessary. Using the following table:

	E_0	E_1	B_1	E_2	B_2
$2s$	-75.211665	0.0	0.020549	-0.006609	-0.000871
$2p^*$	-73.419686	0.0	0.040284	-0.013265	-0.001347

it is possible to calculate the one-particle contributions as

$$E=2\times(2s \text{ contribution})+(2p^* \text{ contribution}).$$

Using Eq. (2.10), the expression for the corresponding $C_{1'1'0 2'2'0 3'3'0}(J'_{12},J''_{12},J)$ coefficient

$$C_{1/2}(ss0p^*)=Q_0(ssp^*)-\frac{1}{\sqrt{2}}Q_0(p^*ss)+\sqrt{\frac{3}{2}}Q_1(p^*ss),$$

and values for two-particle matrix elements,

			E_1	B_1	E_2	B_2
$2s2s$	$2s2s$	$J=0$	3.768813	0.003909	-0.037251	-0.001442
$2s2p^*$	$2s2p^*$	$J=0$	3.292572	0.005144	-0.026257	-0.001810
$2s2p^*$	$2s2p^*$	$J=1$	3.790241	-0.000147	-0.051647	-0.001989

we can calculate the two-particle contributions:

$$E=(2s2s\ \ 2s2s \text{ contr.})+\frac{1}{2}(2s2p^*\ \ 2s2p^*\ \ J=0 \text{ contr.})$$
$$+\frac{3}{2}(2s2p^*\ \ 2s2p^*\ \ J=1 \text{ contr.}).$$

Adding the three-particle contribution from Table I, we then obtain for the $2s^2[0]2p^*$ $[J]$ diagonal matrix element:

Contribution	E_0	E_1	B_1	E_2	B_2
one-particle	-223.84302	0.00000	0.081382	-0.026483	-0.003090
two-particle	0.00000	11.100461	0.006261	-0.127850	-0.005331
three-particle	0.00000	0.00000	0.00000	-0.065637	-0.000214
total	-223.84302	11.100461	0.087643	-0.219970	-0.008634

which gives $E=-212.883\,51$ for the total energy. Results of similar calculations for all 43 second-order energy matrix elements are given in the columns headed $E_1^{(2)}$, $B_1^{(2)}$, $E_2^{(2)}$, and $B_2^{(2)}$ in Table I.

Carrying out the recoupling by this method does not require significant computer time, provided the one- and two-particle contributions are known (as they are in the present case). The only contribution that must be calculated anew is the three-particle diagram. This contribution, however, contains only a single sum over intermediate states, and does not require a lengthy calculation. It should be noted that no additional calculations are necessary to evaluate matrix elements for four-particle systems; it is only necessary to determine the recoupling coefficients C and combine the known one-, two-, and three-particle matrix elements.

After evaluating the energy matrices, we calculate eigenvalues and eigenvectors for states with given values of J and parity. There are two possible methods to carry out the diagonalization: (a) diagonalize the sum of zeroth- and first-order matrices, then calculate the second-order contributions using the resulting eigenvectors; or (b) diagonalize the sum of the zeroth-, first-, and second-order matrices together. Following Ref. [34], we choose the second method here. Second-order Coulomb contributions to the energies are shown in Fig. 2(a) for odd-parity states and in Fig. 2(b) for even-parity states. We see that the energies are smooth functions of Z. It is simple to identify the three doublet states $(2s^2 2p\ {}^2P, 2p^3\,{}^2D, 2p^3\,{}^2P)$ the one quartet state $(2p^3\ {}^4S)$ of odd parity in Fig. 2(a). We see that the splitting of the doublet states is comparable to the difference between LS terms for high Z ions. It should be noted that the second-order energies for odd-parity states are slowly varying functions of Z, ranging from -0.2 a.u. for $Z=5$ to -0.3 a.u. for $Z=100$, for example. Similar comments can be made regarding energies of the even-parity states shown in Fig. 2(b): the energies change, for example, from -0.16 a.u. for $Z=5$ to -0.35 a.u. for $Z=100$. We see that the splitting of the quartet $2p^2 2s\ {}^4P$ term covers almost the entire range of the eight even-parity states (from -0.16 a.u. to -0.45 a.u.). The splitting of the doublet $2p^2 2s\ {}^2D$ term is also large, but the split-

TABLE V. Splitting of the levels for B-like isoelectronic sequence in cm^{-1}.

Z	$2s^2 2p\ ^2P$ (3/2−1/2)	$2p^2 2s\ ^4P$ (3/2−1/2)	$2p^2 2s\ ^4P$ (5/2−3/2)	$2p^2 2s\ ^2D$ (5/2−3/2)	$2p^2 2s\ ^2P$ (3/2−1/2)	$2p^3\ ^2D$ (5/2−3/2)	$2p^3\ ^2P$ (3/2−1/2)
5	17	7	10	0	14	1	2
6	65	24	33	-2	45	-2	3
7	177	62	88	-6	115	-11	6
8	389	134	193	-12	249	-24	12
9	749	258	374	-21	474	-41	25
10	1311	452	659	-30	821	-60	52
11	2140	740	1084	-37	1321	-76	104
12	3309	1152	1685	-37	2002	-77	199
13	4898	1722	2504	-23	2881	-47	365
14	7000	2488	3586	19	3961	40	642
15	9713	3500	4979	108	5218	222	1088
16	13149	4812	6731	270	6601	548	1782
17	17425	6488	8893	541	8028	1088	2826
18	22670	8607	11515	972	9405	1923	4350
19	29022	11256	14643	1628	10645	3150	6515
20	36631	14539	18319	2593	11689	4877	9509
21	45653	18578	22581	3975	12512	7210	13546
22	56260	23509	27455	5907	13112	10250	18861
23	68629	29493	32956	8553	13507	14070	25704
24	82953	36708	39084	12110	13719	18708	34333
25	99423	45354	45818	16806	13776	24150	45007
26	118267	55664	53129	22917	13703	30332	58000
27	139703	67885	60958	30745	13529	37123	73574
28	163972	82295	69235	40632	13278	44347	92002
29	191317	99187	77869	52945	12972	51797	113552
30	222002	118883	86763	68080	12635	59268	138502
32	294498	168060	104929	108456	11929	73604	199751
36	492491	316022	140379	241329	10694	97774	376203
40	779389	551603	172142	465458	9879	116294	642683
42	963920	710787	186428	619880	9602	124047	817319

ting of the doublet $2p^2 2s\ ^2P$ term remains small. The curve for the single doublet $2p^2 2s\ ^2S$ ranges from -0.3 a.u. for $Z=5$ to -0.4 a.u. for $Z=100$. As a result, it is not possible to use the LS designation for high-Z ions; the splitting for these ions is comparable to intervals between the LS terms. We obtain almost pure jj coupling for the highest values of Z.

These observations are confirmed by the Z dependence of the mixing coefficients shown in Fig. 3. This figure shows the mixing coefficients for even parity states with $J=1/2$. There are three states in this complex and their state vectors can be represented in a form

$$\begin{aligned}\Phi(1) &= C_{11}\Phi(2p^*2p^*[0]2s) + C_{12}\Phi(2p2p[0]2s) \\ &\quad + C_{13}\Phi(2p^*2p[1]2s), \\ \Phi(2) &= C_{21}\Phi(2p^*2p^*[0]2s) + C_{22}\Phi(2p2p[0]2s) \\ &\quad + C_{23}\Phi(2p^*2p[1]2s), \\ \Phi(3) &= C_{31}\Phi(2p^*2p^*[0]2s) + C_{32}\Phi(2p2p[0]2s) \\ &\quad + C_{33}\Phi(2p^*2p[1]2s). \qquad (3.1)\end{aligned}$$

The nine coefficients C_{ik} with $i,k=1,2,3$ are shown. We can see from the figure that for small Z (Z = 5 – 17), the largest values are those of the diagonal coefficients C_{11}, C_{22}, and C_{33}. For $Z=18$, the value of the nondiagonal coefficient C_{21} is larger than the value of diagonal one (C_{22}), but this fact does not change the classification of the states ($2p2p[0]2s$) since two other diagonal coefficients (C_{11} and C_{33}) are still larger than their nondiagonal counterparts. The maximum value for C_{21} occurs for $Z=20$, and beyond this maximum the value of C_{21} decreases rapidly. For $Z=20$, the nondiagonal coefficient C_{32} intersects the diagonal one (C_{33}). As a consequence, the state 3 should be designated as $2p2p[0]2s$. For $Z=24$, the nondiagonal coefficient C_{23} becomes larger than other two coefficients C_{21} and C_{22}. This ordering of the coefficients does not change for $Z>24$. In conclusion, we find that, in the interval from $Z=5$–19, the three states of even parity with $J=1/2$ should be labeled as $1=2p^*2p^*[0]2s$, $2=2p2p[0]2s$, $3=2p^*2p[1]2s$ and for $Z>20$ as $1=2p^*2p^*[0]2s$, $2=2p^*2p[1]2s$, $3=2p2p[0]2s$. It should be noted that for a situation where there are almost equal nondiagonal and diagonal coefficients, the names of states in a pure coupling scheme (jj or LS) do not describe these states. It is simple to number them as 1, 2, 3 but then we lose information. Moreover, names of state in

TABLE VI. Energies of even states of boronlike ions given relative to the ground state in eV for ions with $Z=47-100$. Notation: $2p^*=2p_{1/2}$, $2p=2p_{3/2}$.

Z	$2p^*2p^*[0]2s$ 1/2	$2p^*2p[1]2s$ 1/2	$2p2p[0]2s$ 1/2	$2p^*2p[1]2s$ 3/2	$2p^*2p[2]2s$ 3/2	$2p2p[2]2s$ 3/2	$2p^*2p[2]2s$ 5/2	$2p2p[2]2s$ 5/2
47	132.059	360.994	564.159	288.182	358.239	565.287	315.226	501.785
50	145.129	433.954	698.535	357.383	432.422	699.628	386.504	631.367
54	163.158	554.063	922.219	472.162	553.830	923.259	503.790	848.573
60	191.952	794.646	1375.999	704.114	795.757	1376.932	739.030	1292.300
63	207.296	948.094	1668.016	852.982	949.644	1668.883	889.345	1579.093
70	246.240	1415.487	2564.710	1309.037	1417.548	2565.408	1348.281	2462.976
74	270.752	1766.900	3243.577	1653.568	1768.960	3244.179	1694.129	3134.078
79	304.150	2314.779	4306.967	2192.430	2316.562	4307.470	2234.261	4187.246
80	311.157	2440.985	4552.652	2316.776	2442.677	4553.139	2358.808	4430.812
83	333.062	2857.684	5365.183	2727.781	2859.033	5365.639	2770.296	5236.832
90	387.406	4089.473	7778.572	3945.609	4089.629	7779.066	3988.483	7634.039
92	403.659	4521.121	8627.437	4373.090	4520.838	8627.982	4415.842	8478.006
100	469.800	6707.808	12946.594	6542.334	6705.378	12947.620	6583.359	12776.193

the LS-coupling scheme for small Z and jj coupling for large Z are commonly used. For boronlike ions, this problem occurs only for intermediate Z (Z = 18–28).

The final summary of our calculations is given in Tables II–VII and in Figs. 4–6. In these tables, energies are given relative to the $(2s^22p)^2P_{1/2}$ ground state. We use the following notation: $E^{(0+1)}\equiv E^{(0)}+E^{(1)}+B^{(1)}$ is the sum of the lowest- and first-order eneries, $E^{(2)}$ is the second-order Coulomb energy, $B^{(2)}$ is the second-order Breit correction, $E_{\rm Lamb}$ is the QED correction, $E_{\rm tot}$ is the total theoretical energy, $E_{\rm Th}$ is other theoretical data, and $E_{\rm Expt}$ is the experimental energy. The QED contributions were evaluated from one-electron Lamb shift data calculated in a $(1s^2)$ potential following the method described in Ref. [39]. A Fermi distribution with root-mean-square radius from [40] but with thickness $t=2.3$ fm was used to describe the nuclear charge distribution for ions other than U and Th; for these two ions, a nonspherical charge distribution with parameters from Refs. [41,42] was used.

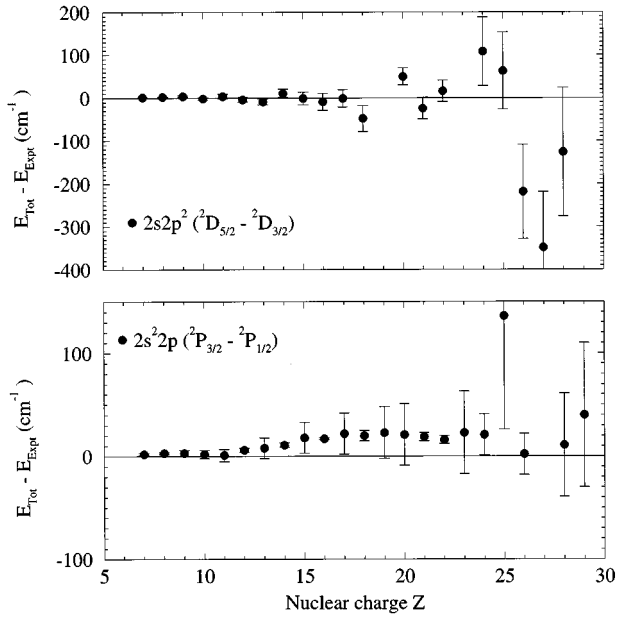

FIG. 4. Difference between theory and experiment for the splitting of $2s^22p\ ^2P$ and $2s2p^2\ ^2D$ levels.

We see from Table II that the second-order Coulomb contribution is still very substantial for intermediate-Z ions, such as $Z=26$. For the $2p^22s\ ^4P$ states of this ion, $E^{(2)}$ is almost equal to $E_{\rm Lamb}$ (with opposite sign), and is 2–5 times larger then $E_{\rm Lamb}$ for all other states except $2s^22p\ ^2P_{3/2}$. Again, for $Z=26$, the second-order Breit contribution is at least nine times smaller than the $E^{(2)}$ for all states except $2s^22p\ ^2P_{3/2}$, for which $E^{(2)}$, $B^{(2)}$, and $E_{\rm Lamb}$ are very close and of the same sign. As Z increases, the relative contribution of the second-order term decreases rapidly (since $E^{(2)}$ is almost constant with Z) and the contribution of the $E_{\rm Lamb}$ becomes 20 times larger than the total second-order contribution for states of boronlike Th and U listed in Table III. We include comparisons with both theoretical and experimental data in Tables II and III.

We will discuss Table II first. The experimental precision is not less than 100–150 cm^{-1} for $2p^22s$ states. Our data are in agreement with experiment within this precision for most of these states. We also compare our results with those obtained by MCDF + nonrelativistic second-order calculations [33]. It can be seen that the present calculations agree better with experiment than do the calculations from [33].

The comparison with experimental data for uranium [8] and thorium [9] and with CI calculations for uranium [35] is given in Table III. For B-like ions two transitions were measured: B-1 from the $(2s_{1/2}2p_{1/2}2p_{3/2})_{3/2}$ state to the ground state, and B-2 from the $(2s_{1/2}2p_{1/2}2p_{3/2})_{1/2}$ state to the ground state. The rows labeled CI-DS and CI-DH are results from large-scale CI calculations using single-particle basis orbitals from Dirac-Slater and Dirac-Hartree potentials, respectively [35]. As can be seen from Table III, the present calculations are in excellent agreement with experiment for all four transitions, and with the CI calculations for uranium ions. It should be noted that the present calculations require considerably less computer time than the CI calculations of Ref. [35].

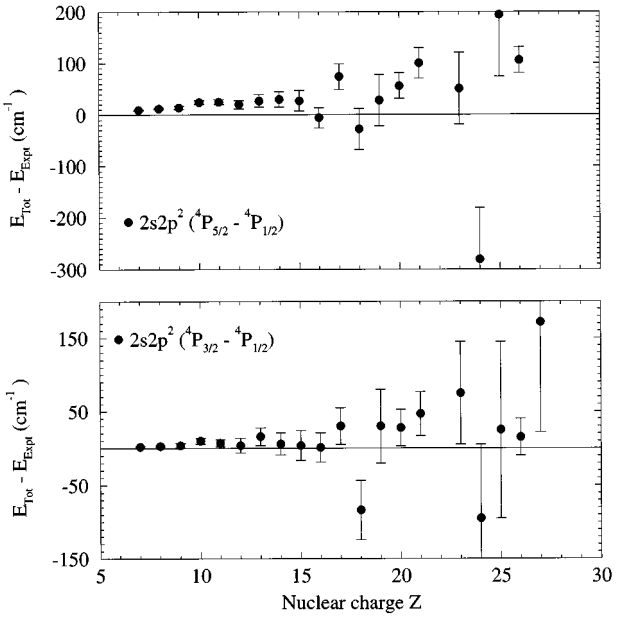

FIG. 5. Difference between theory and experiment for the splitting of $2s2p^2\ ^4P$ levels.

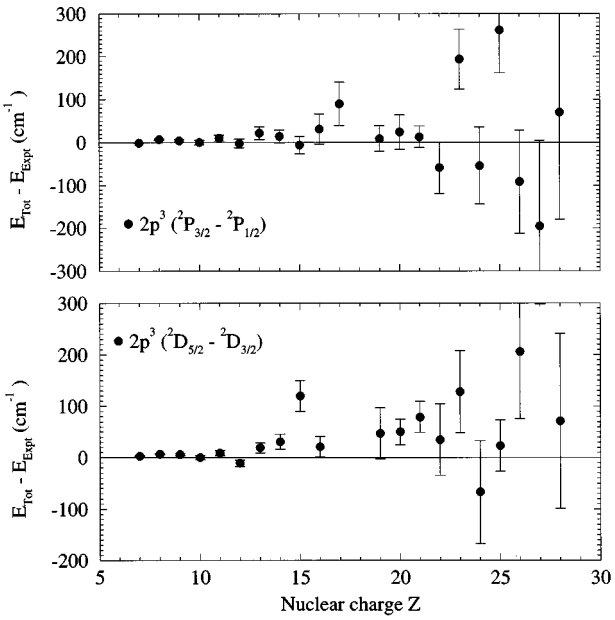

FIG. 6. Difference between theory and experiment for the splitting of $2p^3\ ^2P$ and $2p^3\ ^2D$ levels.

Table IV lists $E_{\rm Tot}$ and $E_{\rm Expt}$ (where available) for 30 ions in the range $Z = 5$–42 for the lowest terms in multiplets, i.e., $^4P_{1/2}$, $^2D_{3/2}$, $^2S_{1/2}$, $^2P_{1/2}$, for even parity states, and $^4S_{3/2}$, $^2D_{3/2}$, $^2P_{1/2}$, for odd parity states. The splitting of $^{4,2}P$ and ^2D terms is given in Table V. It should be noted that the experimental data in Refs. [10–26] for quartet terms ($2s2p^2\ ^4P_J$, $2p^3\ ^4S^{3/2}$) were given with uncertainty $+x$ since there were no observed transitions with $\Delta S = 1$. This uncertainty $+x$ is sometimes the principal contribution to the difference between our results and experimental data (δE). We see, for example, that δE for the $(2s2p^2)\,^4P_J$ and $(2p^3)^4S_{3/2}$ levels changes sharply for $Z = 13$ and 24. For those states with the experimental uncertainty given as $+x$, our theoretical data, which were obtained by one theoretical method for the entire isoelectronic sequence, can certainly be useful. The fact that δE is not a smooth function of Z, for $Z > 20$, can be explained by the varying accuracy of the available experimental data.

The error in the theoretical energy values decreases rapidly from about 1500 cm^{-1} for $Z = 5$ to about 20–500 cm^{-1} for $Z = 20$. The theoretical error for low Z is dominated by the omitted higher-order correlation corrections, which decrease as $1/Z$ of the second-order correlation energy. There is also uncertainty in QED values which contribute to a difference for higher Z.

We obtained very good agreement with experiment for the splitting of all levels: $2s^2 2p\ ^2P(3/2-1/2)$, $2p^2 2s\ ^4P(3/2-1/2)$, $2p^2 2s\ ^4P(5/2-3/2)$, $2p^2 2s\ ^2D(5/2-3/2)$, $2p^2 2s\ ^2P(3/2-1/2)$, $2p^3\ ^2D(5/2-3/2)$, $2p^3\ ^2P(3/2-1/2)$. These splittings are given in Table V for the range of

TABLE VII. Energies of odd states of boronlike ions given relative to the ground state in eV for ions with $Z = 47-100$. Notation: $2p^* = 2p_{1/2}$, $2p = 2p_{3/2}$.

Z	$2p2p[0]2p^*$ 1/2	$2s2s[0]2p$ 3/2	$2p^*2p^*[0]2p$ 3/2	$2p2p[2]2p^*$ 3/2	$2p2p[0]2p$ 3/2	$2p2p[2]2p^*$ 5/2
47	722.788	195.145	503.168	672.603	896.755	690.016
50	870.681	255.722	589.747	817.167	1103.442	835.605
54	1113.050	358.303	728.497	1055.131	1446.012	1074.752
60	1596.575	570.197	998.548	1532.026	2137.828	1553.059
63	1904.325	708.168	1167.559	1836.424	2581.740	1858.001
70	2840.426	1136.117	1674.051	2764.557	3941.639	2786.964
74	3543.646	1462.762	2049.805	3463.118	4969.276	3485.703
79	4639.611	1977.134	2630.552	4553.140	6577.153	4575.618
80	4892.034	2096.356	2763.613	4804.357	6948.372	4826.768
83	5725.418	2491.339	3201.661	5634.092	8175.638	5656.201
90	8188.850	3670.227	4485.860	8088.808	11816.935	8109.601
92	9052.128	4086.394	4933.022	8949.543	13096.661	8969.792
100	13426.078	6212.580	7181.888	13313.078	19602.155	13330.332

$Z=5-42$. The precision of the corresponding experimental data was estimated by Edlén [4]. The difference between the present data and those from [4] (given with error bars) is shown in Figs. 4–6. The best agreement of our data with experimental data was obtained for the splitting of the ground-state multiplet (where the experimental data are very precise). It should be noted that this splitting was measured with better accuracy than the remaining splittings shown in Figs. 4–6. Furthermore, some of the present values of splitting [$(2p^3)\ ^2D$ and $(2p^3)\ ^2P$] were obtained as a result of diagonalization of energy matrices with different J. The splitting for these terms and for the $(2s2p^2)^2D$ term is very small and the sign changes with Z. In such cases, it is very difficult to determine the splitting with high precision; nevertheless, we obtained good agreement (almost everywhere within error bars) with Edlén's experimental data from [4].

In Table VI we present theoretical energies for ions with Z in the range 47–100 for the eight even-parity states. Theoretical energies in this Z range for the seven odd-parity states are presented in Table VII. We use jj-coupling designations in these two tables. The comparison with experiment for $Z=90$ and 92 has already been discussed. We expect that data for other Z will provide a useful guide for future measurements.

In conclusion, we find that MBPT gives excellent agreement with experimental data and with other high-precision theoretical calculations. It would be beneficial if experimental data for other highly-charged B-like ions were available. At the present time, there are no experimental data for ions with Z between 42 and 90. The availability of such data could lead to an improved understanding of the relative importance of different contributions to the energies of highly-charged ions. It would also be useful to have experimental data for other levels of B-like uranium and thorium as well as more precise data for the already measured transitions.

ACKNOWLEDGMENTS

The work of M.S.S. and W.R.J. was supported in part by National Science Foundation Grant No. PHY-95-13179. U.I.S. acknowledges partial support from the University of Notre Dame, Department of Physics. The authors owe a debt of gratitude to J. Sapirstein for supplying values for the QED corrections.

[1] L. A. Vainshtein and U. I. Safronova, At. Data Nucl. Data Tables **21**, 49 (1978); **25**, 311 (1980); U.I. Safronova and R. Bruch, Phys. Scr. **50**, 45 (1994).
[2] M.J. Connely, L. Lipsky, and A. Russek, Phys. Rev. A **46**, 4012 (1992).
[3] B. Edlén, Nova Acta Reg. Soc. Sc. Ups. Ser. IV, **9**, No. 6 (1934).
[4] B. Edlén, Phys. Scr. **28**, 483 (1983).
[5] B. Denne and E. Hinnov, Phys. Scr. **35**, 811 (1987).
[6] J.H. Dave, U. Feldman, J.F. Seely, A. Wouters, S. Suckewer, E. Hinnov, and J.L. Schwob, J. Opt. Soc. Am. B **4**, 635 (1987).
[7] R. Myrnäs, C. Jupén, G. Miecznik, I. Martinson, and B. Denne-Hinnov, Phys. Scr. **49**, 429 (1994).
[8] P. Beiersdorfer, D. Knapp, R.E. Marrs, S.R. Elliott, and M.H. Chen, Phys. Rev. Lett. **71**, 3939 (1993).
[9] P. Beiersdorfer, A. Osterheld, S.R. Elliott, M.H. Chen, D. Knapp, and K. Reed, Phys. Rev. A **52**, 2693 (1995).
[10] Ch.E. Moore, *Atomic Energy Levels*, Nat. Bur. Stand. Ref. Data Ser. No. 35 (National Bureau of Standards, Washington, D.C., 1971).
[11] Ch.E. Moore, *Selected Tables of Atomic Spectra, NIV - NVII*, Nat. Bur. Stand Ref. Data Ser. No. 3, Sec. 4 (National Bureau of Standards, Washington, D.C., 1971).
[12] W.C. Martin and R. Zalubas, J. Phys. Chem. Ref. Data **10**, 153 (1981).
[13] W.C. Martin and R. Zalubas, J. Phys. Chem. Ref. Data **9**, 1 (1980).
[14] W.C. Martin and R. Zalubas, J. Phys. Chem. Ref. Data **8**, 817 (1979).
[15] W.C. Martin and R. Zalubas, J. Phys. Chem. Ref. Data **12**, 323 (1983).
[16] W.C. Martin, R. Zalubas, and A. Musgrove, J. Phys. Chem. Ref. Data **14**, 751 (1985).
[17] W. C. Martin, R. Zalubas, and A. Musgrove, J. Phys. Chem. Ref. Data **19**, 821 (1990).
[18] J. Sugar and Ch. Corliss, J. Phys. Chem. Ref. Data **14**, Suppl. 2 (1985).
[19] T. Shirai, T. Nakagaki, J. Sugar, and W. L. Wiese, J. Phys. Chem. Ref. Data **21**, 273 (1992).
[20] T. Shirai, Y. Nakai, T. Nakagaki, J. Sugar, and W.L. Wiese, J. Phys. Chem. Ref. Data **22**, 1279 (1993).
[21] T. Shirai, T. Nakagaki, K. Okazaki, J. Sugar, and W.L. Wiese, J. Phys. Chem. Ref. Data **23**, 179 (1994).
[22] T. Shirai, Y. Funatake, K. Mori, J. Sugar, W. L. Wiese, and Y. Nakai, J. Phys. Chem. Ref. Data **19**, 127 (1990).
[23] T. Shirai, A. Mengoni, Y. Nakai, K. Mori, J. Sugar, W.L. Wiese, K. Mori, and N. Sakai, J. Phys. Chem. Ref. Data **21**, 23 (1992).
[24] J.R. Fuhr, G.A. Martin, and W.L. Wiese, J. Phys. Chem. Ref. Data **17**, Suppl. 4, 477 (1988).
[25] J. Sugar and A. Musgrove, J. Phys. Chem. Ref. Data **19**, 527 (1990).
[26] J. Sugar and A. Musgrove, J. Phys. Chem. Ref. Data **22**, 1213 (1993).
[27] A.N. Ivanova, U.I. Safronova, and V.V. Tolmachev, Lit. Phys. Sborn. **7**, 571 (1967).
[28] U.I. Safronova and A.N. Ivanova, Opt. Spectrosc. **27**, 193 (1969).
[29] E.P. Ivanova and U.I. Safronova, J. Phys. B **8**, 1591 (1975).
[30] U.I. Safronova and V.N. Kharitonova, Opt. Spectrosc. **28**, 1039 (1970); U.I. Safronova, *ibid.* **28**, 1050 (1970); **33**, 813 (1972).
[31] U.I. Safronova, J. Quantum. Spectrosc. Radiad. Trans. **15**, 231 (1975).
[32] K.T. Cheng, Y.K. Kim, and J.P. Desclaux, At. Data Nucl. Data Tables **24**, 111 (1979).
[33] K.T. Cheng, C. Froese Fisher, and Y.-K. Kim, J. Phys. B **15**, 181 (1982).
[34] M.S. Safronova, W.R. Johnson, and U.I. Safronova, Phys. Rev. A **53**, 4036 (1996).

[35] K.T. Cheng and M.H. Chen, Phys. Rev. A **53**, 2206 (1996).
[36] U.I. Safronova and Z.B. Rudzikas, J. Phys. B **9**, 1989 (1976).
[37] D.A. Varshalovich, *Quantum Theory of Angular Momentum: Irreducible Tensors, Spherical Harmonics, Vector Coupling Coefficients, 3nj Symbols* (World Scientific, Singapore, 1988).
[38] W.R. Johnson, S.A. Blundell, and J. Sapirstein, Phys. Rev. A **37**, 2764 (1988).
[39] K.T. Cheng, W.R. Johnson, and J. Sapirstein, Phys. Rev. A **47**, 1817 (1993).
[40] W.R. Johnson and G. Sofft, At. Data Nucl. Data Tables **33**, 405(1985).
[41] J.D. Zumbro, E.B. Shera, Y. Tanaka, C.E. Bemis, Jr., R.A. Naumann, M.V. Hoehn, W. Reuter, and R.M. Steffen, Phys. Rev. Lett. **53**, 1888 (1984).
[42] J.D. Zumbro, R.A. Naumann, M.V. Hoehn, W. Reuter, E.B. Shera, C.E. Bemis, Jr., and Y. Tanaka, Phys. Lett. **167B**, 383 (1986).